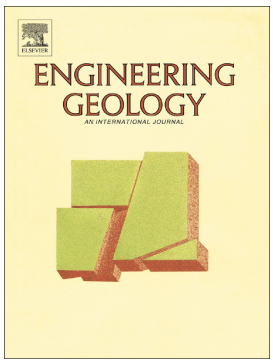


# Geophysical reconstruction of buried geological features and site effects estimation of the Middle Valle Umbra basin (central Italy)

Daniela Famiani, Carlo Alberto Brunori, Luca Pizzimenti, Fabrizio Cara, Marco Caciagli, Laura Melelli, Francesco Mirabella, Massimiliano R. Barchi

PII: S0013-7952(19)31245-1

DOI: https://doi.org/10.1016/j.enggeo.2020.105543

Reference: ENGEO 105543

To appear in: *Engineering Geology*

Received date: 27 June 2019

Revised date: 4 February 2020

Accepted date: 18 February 2020

Please cite this article as: D. Famiani, C.A. Brunori, L. Pizzimenti, et al., Geophysical reconstruction of buried geological features and site effects estimation of the Middle Valle Umbra basin (central Italy), *Engineering Geology* (2020), https://doi.org/10.1016/j.enggeo.2020.105543

# Geophysical reconstruction of buried geological features and site effects estimation of the Middle Valle Umbra basin (central Italy).

Daniela Famiani[1], Carlo Alberto Brunori[1], Luca Pizzimenti[1], Fabrizio Cara[1], Marco Caciagli[2], Laura Melelli[3], Francesco Mirabella[3] and Massimiliano R. Barchi[3]

[1]Istituto Nazionale di Geofisica e Vulcanologia, Sezione di Sismologia e Tettonofisica, Roma

[2]Istituto Nazionale di Geofisica e Vulcanologia, Sezione di Sismologia e Tettonofisica, Bologna

[3]University of Perugia, Department of Physics and Geology (Perugia, Italy)

*Corresponding author*: Daniela Famiani (daniela.famiani@ingv.it)

## Abstract

The Middle Valle Umbra (central Italy) is a NW-SE 20 km long and 10 km wide Quaternary extensional basin located in the internal sector of the Apennine chain. This area historically experienced strong earthquakes that caused significant damages to the outstanding historical heritage. The same area has been recently hit by the 2016 seismic sequence of Amatrice-Visso-Norcia.

With the aim to reconstruct the buried geological structures of the basin, a multi-technique geophysical approach was performed. An extended campaign of ambient noise measurements was carried out to investigate the subsurface setting, and to identify the main geological units. We performed three 2D passive arrays to analyze two different sites within the basin; their aperture was between 150 and 752 m for one site and of 48 m for the other site, to characterize the geological units in terms of sediment thickness and shear-wave velocity profile. Data collected were processed with f-k and MSPAC analysis to extract dispersion curves with good resolution in a frequency range of 0.5-10 Hz and 4.5-18 Hz for the two sites respectively. Spectral ratios were computed for every single station ambient noise measurement performed and for all the stations of the bigger array. Our final target is to extend these results to the whole valley, in order to retrieve the attitude of the main geological units and propose a reliable reconstruction of the subsurface geometry of the basin. Another point of this work is to evaluate the site response in the middle of the valley through the analysis of the earthquakes recorded by the accelerometric station IT.CSA (belonging to the Italian Civil Protection) and the corresponding recordings of the nearby rock station IT.ASS.

**Keywords:** site effects, seismic site characterization, subsoil model, Valle Umbra, spectral ratios, passive arrays

## 1. Introduction

The Valle Umbra basin is a large inter-mountain Quaternary extensional basin located in the northern Apennines (Italy) (Fig. 1). The object of this paper is the middle part of the Valle Umbra basin (hereinafter MVUB), delimited by the Tiber river valley to the north (where the town of Perugia is located), the village of Assisi to the east, Foligno and Bevagna to the south

and Cannara in the west. The MVUB is characterized by thick Late Pleistocene-Holocene alluvial deposits (down to a depth of about 150-200 m) overlying the Late Pliocene-Pleistocene continental sequence infilling the basin (Bevagna Unit) which is estimated to be thicker than 600 m. This general geological setting is expected to have a large variability along the basin in terms of thickness and mechanical properties. It is important to note that in particular during the last decades the MVUB has been subject to an intense exploitation of deep water that is producing a rapid compaction and consequent subsidence of the unconsolidated sediments at the surface (Guzzetti et al. 2009, Brunori et al. 2018).

As evinced from the Parametric Catalogue of Italian Earthquakes 2015 (CPTI15; Rovida et al., 2016), the Valle Umbra basin was struck by historical events (1352, 1832, 1854, 1865, 1878 and 1917 in Fig. 1) with macroseismic intensity > VII that caused several casualties and damage. Recently the MVUB was also affected by the 1997 Colfiorito earthquake (M 6.0) and, more marginally, by the very long seismic sequence of Amatrice-Visso-Norcia (main shock, Norcia, PG, Mw 6.5, 30 October 2016). Since 1986, the Italian Civil Protection installed two accelerometric stations in the valley, the IT.CSA station in the middle of the valley and IT.ASS station in the eastern side of the valley in the Assisi village. Therefore, nowadays there is a good database of digital earthquake recordings that comprises a wide range of magnitudes (M > 3.5).

Summarizing, at least three issues make the MVUB an important area to be studied in detail from a seismological point of view: 1) the area is subject to strong earthquakes coming from different active faults; 2) the area is highly vulnerable because there are several towns and villages built in the middle ages and founded in Roman times or, previously, by the Etruscans or the Umbrians (e.g. Assisi, Foligno, Bevagna) which host plenty of monuments and artworks that need to be preserved; 3) during earthquakes, the geological setting (soft soils over stiffer units) is prone to produce amplification effects which are largely unknown in detail.

The presence of structures cutting the bedrock buried under quaternary and recent deposits was investigated using different techniques such as the analysis of subsidence phenomena deforming unconsolidated valley deposits by means InSAR data (Murgia et al., 2019), or by the joined analysis of damage scenario in Roman archeological site and the interpretation of valley morphologies by means of a Digital Elevation Model study (Cinti et al., 2015).

The aim of this paper is twofold: a) to characterize the recent sedimentary infill in terms of geometry (thickness) and shear-wave velocity; b) to evaluate the empirical site response of the area where the station IT.CSA is installed.
Point a) is addressed through several techniques: first, we analize a detailed ambient vibration survey along the valley in order to characterize the basin in terms of resonance frequency using the horizontal-to-vertical spectral ratio (hereinafter HVNSR) technique; second, we perform three 2D passive arrays of seismic stations to evaluate the shear-wave velocity profiles associated to the two areas of investigation. By integrating the results coming from HVNSR and the velocity profiles from passive arrays with the a-priori information about the outcropping geological units and few borehole logs we produce a new and detailed reconstruction of the overall geometry of the basin.
Point b) is tackled through the analysis of the earthquakes recorded by the station IT.CSA and the simultaneous recordings in the closest rock site with respect to IT.CSA, that is the station installed at Assisi and called IT.ASS. For the analysis of the earthquakes we use both the horizontal-to-vertical (hereinafter HVSR) and the site-to-reference spectral ratio (hereinafter

SSR) techniques. In particular this latter technique after a careful check of the background assumptions and the goodness of the reference site, is believed to provide the best estimation of the empirical amplification curve for a site. We finally compare and discuss the average HVSR, the average SSR curve with the SH transfer function obtained using the velocity model coming out from the 2D passive array performed at CSA.

The paper is organized as follows: first, we introduce the geological setting and the historical and recent seismicity of the area; second, we describe both the experiments, the geophysical approaches and analyses performed in the MVUB. Then, we discuss the obtained results and finally combine them with other information available to get a coherent model of the subsurface geology of the area.

## 2. Geological and geomorphological setting

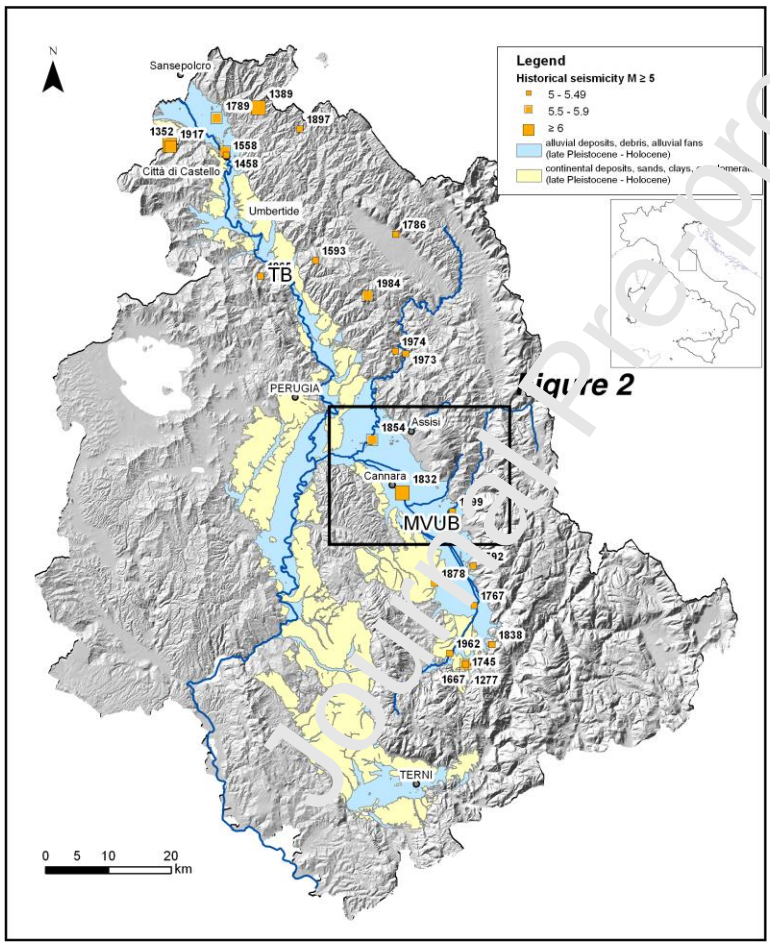


**Figure 1 - General setting of the Middle Valle Umbra basin (MVUB) in the framework of the Quaternary deposits of Tiberino basin (TB). Historical seismicity occurring along the Valle Umbra basin is reported with orange squares proportional to the intensity of the earthquake.**

The Valle Umbra intermountain basin (hereafter UV) is 50 km long, with a NNW-SSE trending alignment of extensional faults, crossing the Umbria region from North to South. The UV is the eastern segment of the Tiberino Basin (TB), the largest of the intermountain basins in the Umbria region (with an area of about 1800 square kilometers, Fig. 1). The TB crosses entirely the region from the north (Sansepolcro) to the south with an overturned Y shape, splitting close to Perugia into two segments. The western branch is elongated southwards up to the city of Terni while the eastern one is the UV (Ambrosetti et al., 1995; Basilici, 1997).

The TB is active since Late Pliocene and is bounded by a complex segmented system of both ENE-dipping and WSW-dipping normal faults, dissecting the pre-existing (Late Miocene) compressional structures of the Umbria-Marche Apennines (e.g. Malinverno and Ryan, 1986; Martini and Sagri, 1993; Barchi, 2010). Some of these faults are still active and seismogenic, as suggested by the distribution of both instrumental and historical seismicity (Rovida et al., 2016). Geodetic data depict the strain field active in this region, with WSW-ENE extension rate of about 3 mm/yr, coherently with the focal mechanisms of the instrumental seismicity (D'Agostino et al., 2001; Pondrelli et al., 2006; Anderlini et al., 2016; Devoti et al., 2017). Extensional tectonics

interacts with a regional uplift in the order of ~ 0.5 mm/yr, which has affected the area since about 1.5 Myr (Ambrosetti, 1982; Cinque et al., 1993; D'Agostino et al., 2001; Mariani et al., 2007). This interaction is such that actively subsiding basins do not always coincide with the active depocenters, depending on the balance between the efficiency of the basin-bounding faults in producing subsidence and the regional uplift. Where normal faults are efficient in producing subsidence at rates larger than the regional uplift, mainly aggradation occurs. Conversely, where normal faults are active but their vertical component rate is lower than the regional uplift, incision prevails (Melelli et al., 2014; Pucci et al., 2014).

The Late Pliocene-Pleistocene continental sequence infilling the Valle Umbra basin consists of a complex succession of laterally discontinuous deposits, mainly composed of lignitiferous clays, sands, sandy clays and conglomerates, deposited within the "ancient Tiberino lake" (Albani, 1962), a depositional environment characterized by braided rivers and shallow lakes (Conti and Girotti, 1977; Ambrosetti et al., 1987; Barchi et al., 1991; Basilici, 1997; Coltorti and Pieruccini, 1997; Martinetto et al., 2014; Bucci et al., 2016). In the following, we will refer to this complex succession as the "Tiberino Lake Succession" TLS. The TLS uncomfortably overlies a previously deformed and eroded bedrock, mainly consisting of Late Miocene turbidites of the Marnoso-Arenacea Fm. (hereinafter MA, Ricci Lucchi, 1986) or, locally, of the older Mesozoic-Paleogene Umbria-Marche multilayer (hereinafter UCM, e.g. Cresta et al., 1989). Along the present-day alluvial plains of the Valle Umbra basins, the TLS is unconformably overlain by Late Pleistocene-Holocene alluvial gravel and sands, more directly referable to the activity of the present-day fluvial network: at the connection with the slopes bordering the valley, the clastic sediments of the alluvial plain are laterally inter-fingered with coarser alluvial fan deposits, larger and more frequent on the NE side of the basins. The thickness of the recent alluvial deposits is quite irregular, varying from few meters up to about 200 m in the deepest depocenters, highlighting significant longitudinal variations of subsidence and activity (Mirabella et al., 2018).

The arrangement of altitude values and the pattern of the drainage network are useful geomorphological evidences to highlight the contribution of the tectonic control vs. the most recent man-made changes on the area (Figs. 1 and 2). The flat alluvial plain, gently decreases northward from about 300 m a.s.l. on its southern limit close to Spoleto to about 170 m a.s.l. at the confluence between the Chiascio and the Tiber rivers, with an average slope value less than 0.3°. The flow direction is to the north, showing an opposite trend with respect to the entire TB where the Tiber river flows from north to south. In the southern part of the UV, both the main rivers (Marroggia and Clitunno) and their tributaries flow northward parallel to each other, inside straight and narrow artificial banks. The fluvial system shows a sediment regime with historical and morphological evidences of overflowing events. Close to Foligno, where the Topino river enters into the UV creating a large alluvial fan, the main rivers are shifted towards the left side of the valley. This asymmetry is due both to the activity of the faults and to the progradation of the fan, and persists until the basin closure near Torgiano. Near Cannara the Topino river collects the waters of the drainage network coming from the south, highlighting an elbow curve at the confluence point repeated by the Chiona river too. Further north, the Tescio river has an irregular confluence with a perpendicular angle. Finally, the segment of Chiascio river immediately before the confluence in the Tiber one is quite anomalous as it traces a wide curve close to Torgiano village. Along the basin, SW-dipping normal faults segments cut the upper and middle portions of the alluvial fans, showing three different behaviors, driven by the interaction between drainage river activity and tectonics. The Topino alluvial fan is wide and low-lying with uncertain limits along the

lower fan segment, due to the strong vertical and lateral interaction with the recent alluvial deposits. The alluvial fan of the Chiascio river on the contrary is active only in the upper fan segment due to the total burial of the fan from the alluvial deposits of the Tiber river. Finally, the Tescio alluvial fan (close to Assisi) is characterized by coarse sediments with a steeper slope but a very low degree of organization (Cattuto et al., 2005). Even if these landforms show clear differences in their geometry and evolution, they were a sort of drainage divide inside the basin favoring swampy areas as in the case of the Topino alluvial fan that was in the past a natural barrier for the rivers flowing from Spoleto.

The human influence during the most recent historical events is a crucial point for understanding the current state of the area. The low-lying morphology and the high drainage density attracted in the past important human settlements. In the same time however, these conditions triggered flooding events and, as a consequence, the past civilizations needed to reclaim the territories (Radmilli, 1960; Barker, 1984). In the pre-roman age, a large lacustrine area (the *Lacus Umber*), covered the northern and central part of the basin up to 219 m a.s.l. In the Roman period (753 BC - 476 AD) the growing of infrastructures as important roads and towns prove better climatic and environmental conditions. The decrease in average rainfall values led to a lowering of the lake level together with the rise of alluvial fan deposits acting as a drainage divide inside the valley. In the historical maps dated 1727 (Cadestre "Chiesa") both the Tiber and the Chiascio rivers highlight a very different pattern with meanders and abandoned channels due to the different base levels imposed by the lacustrine area. The Torgiano ridge is a topographic evidence of the presence of transversal (i.e. NE-SW trending) faults, creating a natural barrier to the rivers flowing northwards and the main cause of the *Lacus Umber*. The thickness of both TLS and Late Pleistocene and Holocene alluvials decrease abruptly along this threshold proving a drop of the basin subsidence in this area. In this paper, we focus on the MVUB, in the central part of UV (Figs. 1-2). Here, the basin is bordered by opposite-dipping normal faults, with markedly different morphology and tectonic setting. The NE flank of the basin is bounded by the relatively high and steep relief of M. Subasio, an anticline culmination where the UCM crops out. The base of the slope is characterized by a set of stepped, SW-dipping normal faults, where an intermediate fault block is characterized by the outcropping middle-upper Miocene Marnoso-Arenacea formation (MA). The shallowest SW flank corresponds to the NE slope of the Martani Mountains, where the bedrock consists of MA. Between the bedrock and the flat floor of the basin, a strip of TLS is exposed, made of Early Pleistocene sandy clays with lignite beds and sandy layers of a flood-plain, fluvial-lacustrine and alluvial fan-delta depositional environment (Bevagna Unit, Bizzarri et al., 2011; 2018). South of the study area, these deposits are overlaid by a conglomerate sequence, forming the Montefalco hill (Gregori, 1988; Mirabella et al., 2018). About 15 km south of the study area, high resolution seismic reflection profiles revealed the presence of NE-dipping low-angle normal faults, separating the present-day alluvial floor of the basin from the hilly landscape of the Pleistocene succession (Mirabella et al., 2018; Barchi and Lemmi, in press).

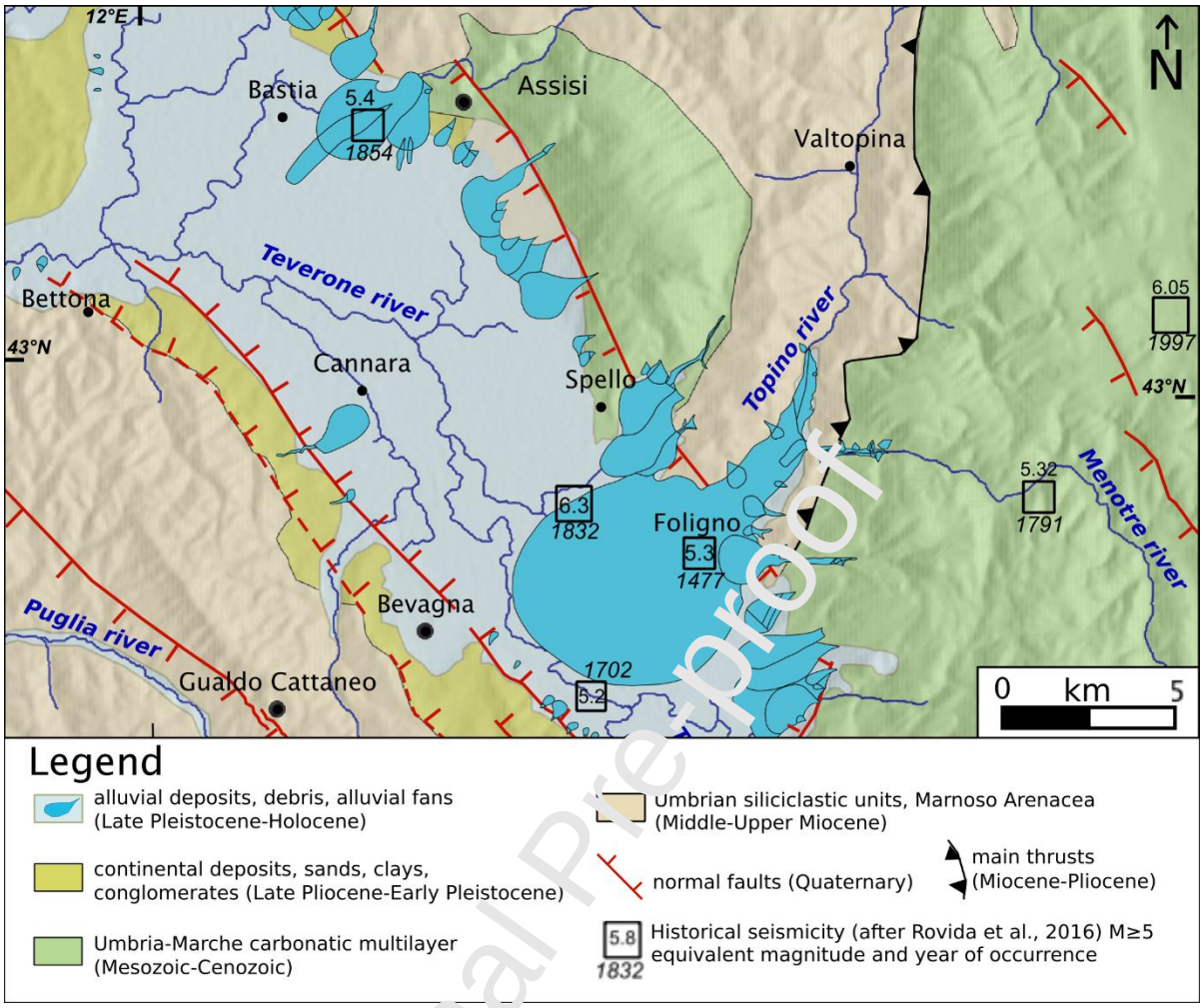


**Figure 2 - Geological framework of the MVUB and historical seismicity.**

The basin is infilled with a thick sequence of recent (i.e. Late Pleistocene-Holocene) alluvial deposits and characterized by the absence of river terraces suggesting that the valley is actively subsiding, despite the regional uplift of the Apennines (Mirabella et al., 2018). A set of water wells, drilled about 3 km NW of Cannara (Fig. 2) encountered the bottom of the recent alluvials at a depth of about 150 m (Saccucci, 2011; Beretta et al., 2018). Other wells, located along the same valley South of Foligno (AA.VV., 1991; Barchi and Lemmi, in press), drilled a comparable thickness (up to 200 m) of alluvial deposits. The Cannara wells show that the recent alluvial deposits consist of a complex, both vertically and laterally heterogeneous assemblage of lens-shaped both coarse (sand and gravel) and fine (silt and clay) sedimentary bodies, with coarser ones tracing the position of ancient river channels. The Cannara wells also reveal that the alluvial deposits overlie consolidated "blue" sandy clays, similar to the TLS succession (Bevagna Unit) exposed along the SW flank of the valley. Based on the available geophysical data, including also geo-electrical and seismic reflection surveys (Ge.Mi.Na., 1962; Barchi et al., 1991; Giaquinto and Martinelli, 1991; Barchi and Lemmi, in press), the maximum thickness of the TLS succession beneath the Valle Umbra basin is estimated to be over 600 m. The deepest part of the TLS succession, directly overlying the bedrock, could comprise also older (i.e. Late Pliocene) fluvio-lacustrine

deposits, presently exposed at the southern end of the basin, near Spoleto (Morgano Unit), hosting mammal fauna dated to about 3.3–3.1 Ma (Triversa faunal unit: Petronio et al., 2002; Argenti, 2004).

## 3. Seismicity of the area

The Parametric Catalogue of Italian Earthquakes 2015 (CPTI15; Rovida et al., 2016) reports that the entire Valle Umbra area was struck by historical seismicity with macroseismic intensity > VII, mainly located on the eastern edge of the valleys (Fig. 1). Nevertheless, there are seismic events, such as the 1352, 1832, 1854, 1865, 1878 and 1917, with macroseismic epicenters located on the western edge and along the valley.
Some of the geological sources responsible for the historical seismicity are still discussed in the literature. According to the recent observed seismicity (Pondrelli et al., 2006), the most energetic historical events that occurred on the eastern edge, may be reasonably associated with SW-dipping and NW-SE-trending active normal faults (Lavecchia et al., 1994; Barchi et al., 1998; Boncio et al., 2004; Basili et al., 2008; Barchi and Mirabella, 2009).

Focusing on the MVUB, the occurrence of seismic events in this area, in particular in the 19th century, suggests that the seismic sources which can be revealed by our investigation could be the same seismic sources also of the historical earthquakes hitting the MVUB described in the CPTI15 and DISS databases. In particular, the January 13, 1832 event represents the most energetic earthquake (M 6.4) that struck the valley. This earthquake was the main-shock of a seismic sequence begun in 1831, with two main events occurred on October 27 and November 6 and continued at least until the end of 1832 with the most energetic earthquake occurred on April 19, 1832 (Guidoboni et al., 2018). Both the foreshocks and aftershocks damaged mainly the villages on the south-eastern edge of the valley and, in particular, the village of Foligno and the surrounding area (Guidoboni et al., 2018). The Database of Individual Seismogenic Sources (DISS WG, 2018) associates the M 6.3 event to a blind NE-dipping and NW-SE-trending normal fault.

As regards the instrumental seismicity, the study area is at an epicentral distance of around 20 and 45 km respectively from the mainshocks of the 1997 Colfiorito and the 2016-2018 Central Italy seismic sequences, recording PGA values of 168.815 and 75.034 cm/s$^2$ at IT.CSA accelerometric station installed in Cannara municipality (PG) attesting that the area suffered from recent relevant shaking.

## 4. Experiment

### 4.1. Noise measurements

In the literature there are several papers that highlight the advantage to use the ambient noise wavefield with respect to other cost-consuming and invasive geophysical techniques for site characterization. Starting from Nogoshi and Igarashi (1971) and widely after the seminal paper of Nakamura (1989), the basic assumption is that the main frequency peak of the horizontal-to-vertical spectral ratio on noise (HVNSR) coincides fairly well with the fundamental resonant frequency of the given site. In the hypothesis that the noise wavefield mainly consists of body waves there is a linear relationship that links the fundamental frequency with the shear wave velocity and the thickness of the layer that produces that resonance.

The seismological community largely debated about the real constitution of the noise (Bonnefoy-Claudet, et al., 2006). In most theoretical model for H/V interpretation, the surface waves, in particular Rayleigh waves, dominate (Yamanaka et al. 1994, Fäh et al. 2001, Bonnefoy-Claudet et al., 2006). The assumption is valid because most of the seismic energy from a point source is radiated as Rayleigh wave (Miller and Pursey, 1955). In that case the peak on HVNSR should be related to the ellipticity of Rayleigh waves. Recently, new theoretical developments emerged using interferometric principle under diffuse field assumption as the base to explain the full spectrum of the microtremor horizontal-to-vertical spectral ratio (Sánchez-Sesma, F.J. et al., 2011, Kawase et al., 2015, Lontsi et al., 2019). Independently of the physical model about the nature of noise, the occurrence of frequency peaks on HVNSR of amplitude greater than 2 is mostly indicative that there are important impedance contrasts at depth (Lachet and Bard, 1994, Lermo and Chávez-García 1994).

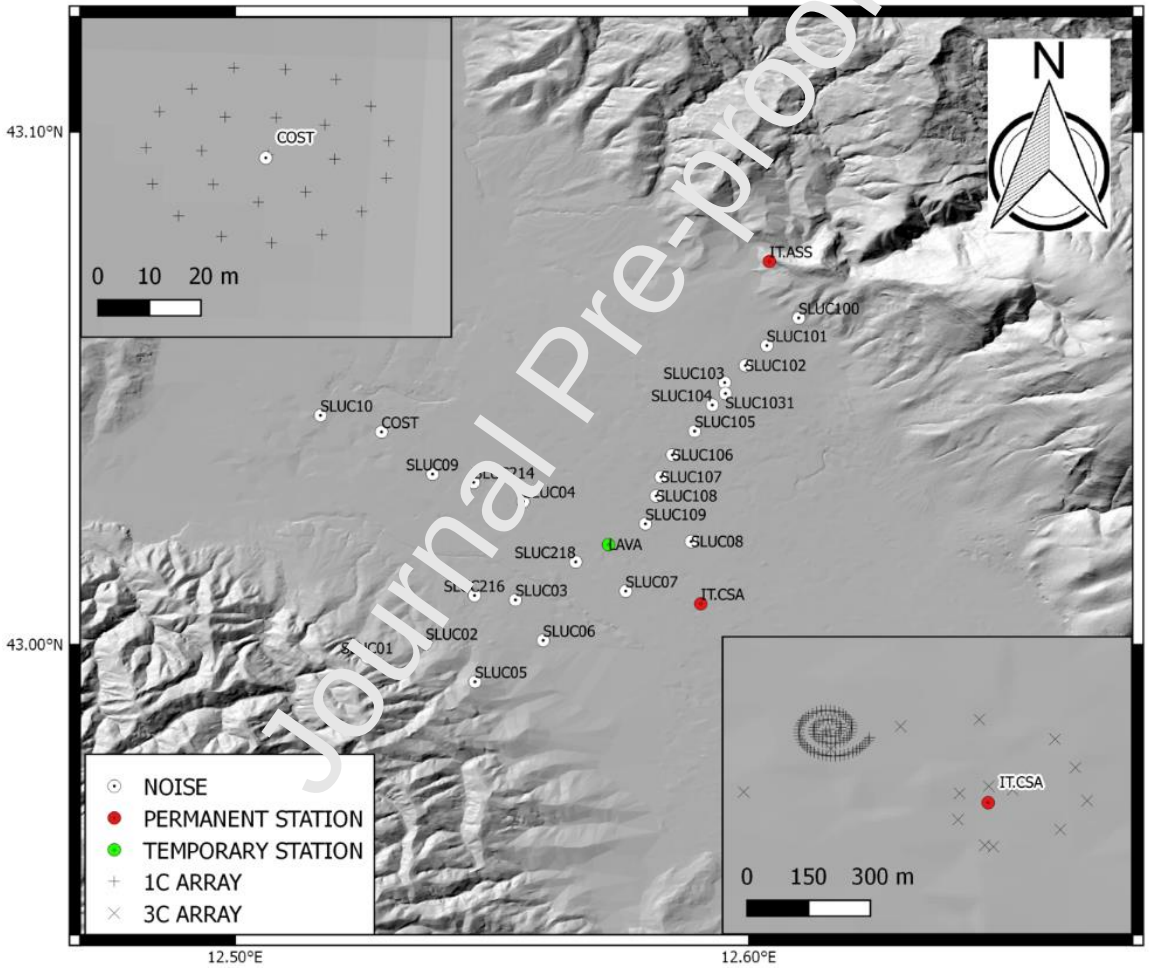


With this idea in mind, the first step of our work was to perform a wide campaign of single-station ambient noise measurements all over the MVUB to get general information about the main impedance contrasts of the subsoil. Single-station ambient noise spectral ratios were organized in transects oriented along the main elongation of the basin and

**Figure 3 - Location map of the geophysical surveys. The main panel shows the points of the microtremor survey (white dots), the temporary station (green dot) and the accelerometric stations considered for earthquake analysis (red dots). The two zooms in the corners show the geometry of the arrays carried out for CSA (bottom right) and COST (top left) sites. The hillshade in background is obtained from TINITALY 10-m-resolution Digital Elevation Model (Tarquini et al., 2007)**

perpendicular to it.

The SW-NE transect is transversal to the basin axis and is composed by 17 stations while the NW-SE transect follows the elongation of the valley and is composed by 9 stations.

Each single station acquired at least 1 hour of ambient noise. An anti-trigger algorithm was applied on the continuous recording and we selected a large number of 40 seconds length time windows not affected by transients. The time windows were detrended and 5% cosine tapered. The Fourier transform was applied to the three components of each window and spectra obtained were smoothed with a Konno-Ohmachi algorithm with constant b=40. Then the spectra of the two horizontal components were combined into

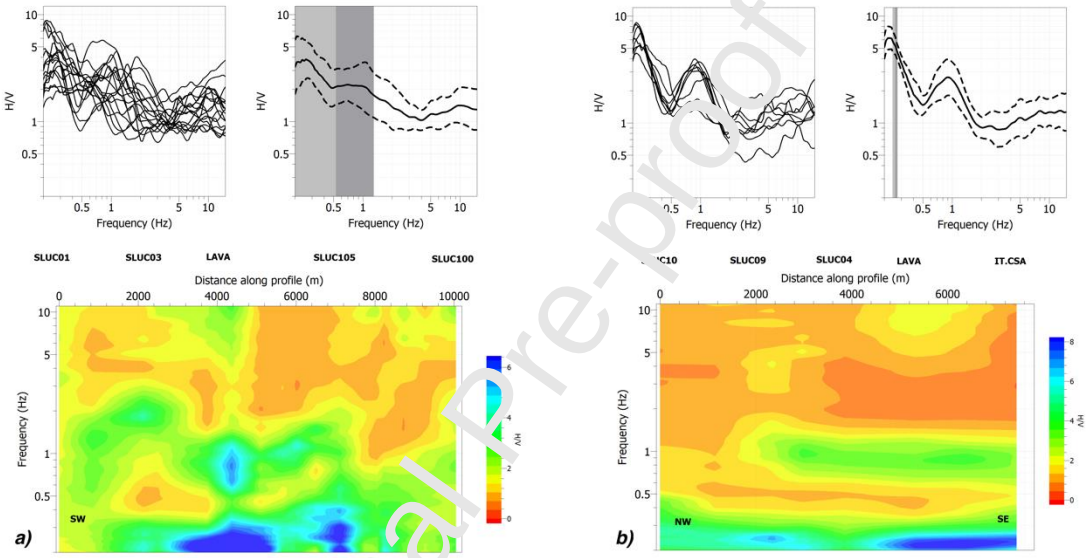


quadratic mean before dividing by the vertical component. The final geometric mean of the HVNSR and standard deviation were obtained by averaging the H/V ratios from all windows.

Top panels of Figure 4a and 4b show the plot of all the HVNSR curves (left side) and the average of all (right side), highlighting a general predominance of two peaks, the lowest one at around 0.2-0.3 Hz and the second close to 1 Hz. This reflects the presence of two main impedance contrasts moving along the transect. The lowest part of the figure shows the contour plots of the HVNSR results along the two transects: this kind of representation is aimed to enhance the perception of the trend of subsoil impedance contrasts and to give them a geological connotation. From the comparison of the two transects, it is possible to note that the transversal transect (Fig. 4b) highlights more spatial variations in the resonant frequencies and the associated amplitudes, while the longitudinal one (on the right) shows more regular trends. Between 3000 m and 7500 m from the beginning of the SW-NE transect (Fig. 4a) there is also an increase of the amplitude values of the peaks, especially the fundamental ones. This is better shown in Fig. 1a-b of Supplementary Materials which reports single HVNSR curves sorted from

**Figure 4 - HVNSR ambient noise measurements, collected along a SW-NE trending transect (a) and a NW-SE (b). a-b) Top: plot of HVNSR curves (left plot) and average of all (right plot); a-b) Bottom: contour plot of the HVNSR curves of each station aligned along the profile of the two transects with the position of some stations as reference (see Fig. 3 for the location of all the stations).**

the westernmost to the easternmost station for both transects.

### 4.2.The problem of the low-frequency

The first frequency peak showed by the HVNSR curves (0.2-0.3Hz) is close to the corner frequency of the sensors used for our noise measurements. In order to assure that this peak is really physical and not due to the instrumentation, we decided to install for 2 weeks a seismic station equipped with a Trillium compact 120s, a broad band velocimeter, in the central part of the MVUB. We called this site LAVA.

Besides the check of the reliability of the low frequency peak in HVNSR, the noise recordings at LAVA allow also to highlight the variations of the day/night noise level as well as the contribution of anthropogenic activities to the noise wavefield.

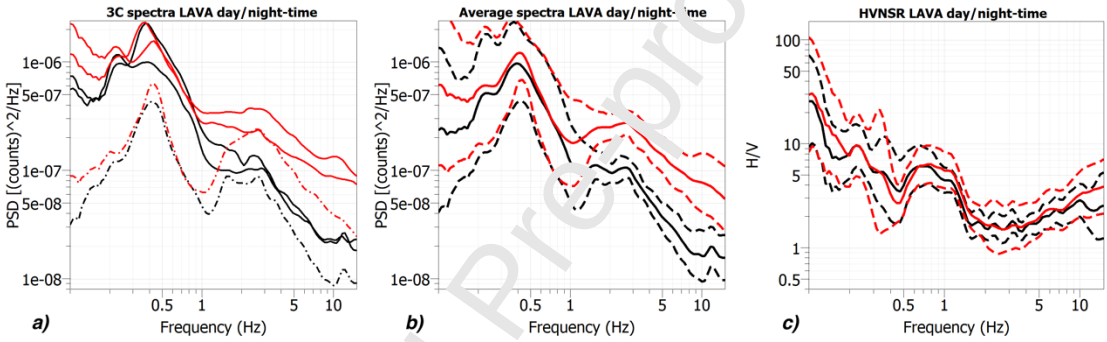


**Figure 5 - Spectra and HVNSR analysis of 12 h of broad-band continuous recording at LAVA site during day-time (red curves) and night-time (black curves). a): spectra of the 3 components (horizontal with solid line and vertical with dotted line) of the LAVA broad-band station during day and night time; b): average spectra (solid lines) and their standard deviations (dashed lines) for the day and night time intervals; c): average HVNSR (solid lines) and their standard deviations (dashed lines) of day and night time intervals where the 0.25 Hz peak results well defined and therefore reliable as a resonance peak for the site.**

Within the 2 weeks of noise recordings, we selected 60 s night-time windows from midnight to 4 am UTC and 60 s day-time windows from 11 am to 3 pm UTC for 3 days. We also performed HVNSR on both the selected data windows to verify possible influences of the different levels of noise on all the investigations we performed during day-time (Fig. 5).

If we focus on the 3-components spectra and the average spectra (Fig. 5a-b) we can clearly observe the large amplitudes of the curves for the daily intervals compared to the night ones, especially above 1 Hz. This is quite trivial because included in the frequency range of the anthropic noise (Bonnefoy-Claudet, et al., 2006). Nevertheless, from the comparison of HVNSR curves on the two different time windows, we can state that the anthropic noise produced in the area of the LAVA site during day-time does not

significantly affect the average HVNSR curves (Fig. 5c), especially in our frequency range of interest.

This is an important result that we believe can be extended for the entire study area, being the LAVA site representative of the level of noise of the MVUB.

To explore the identity of the noise wavefield for the site, under the diffuse field assumption, we inverted HVNRS curve by using HVInv code (Garcìa-Jerez et al. 2016). The part of the curve inverted is included between 0.2 and 1.8 Hz (the frequency range for which the HVNSR curve is involved during the inversion process; see Section 4.3.1). We performed two inversions changing the wave parametrization as follows: the first inversion was made considering a wavefield characterized by 5 modes of Rayleigh and 5 modes of Love waves, while in the second inversion we constrained the wavefield to be composed only by 3 modes of Rayleigh waves and no contribution of Love waves. The results of the two inversions show that the influence of the Love waves in the HVNSR curve mainly affects its amplitude, preserving quite well the values of the frequency peaks (see Fig. 2 of Supplementary Materials for the results of the inversions) suggesting a minimum contribution of Love waves in the noise wavefield at these frequencies.

As regards the fundamental resonance peak at 0.73 Hz, HVNSR performed for the station LAVA (Fig. 5c) shows that it is well defined also in its left side, leaving any doubts about its reliability as representative of the subsoil.

### 4.3. 2D passive arrays

The 2D passive arrays is a widely spread technique to get information on thickness and shear-wave velocity of the layers at depth. It is based on the simultaneous recordings of ambient noise by a number of seismic stations deployed in a chosen 2D configuration in an area, which is expected to have a quite uniform geological setting. The maximum distance (or aperture) between couple of stations infers the investigation depth, but this latter quantity also depends by other parameters, in general it is between a quarter and a half of the aperture. The minimum distance between couple of stations determines the resolution of the array, which is the maximum frequency that can be detected by the array. The hypothesis of the method is that the stations record ambient noise mostly composed by surface waves which are dispersive, meaning that their velocity is frequency dependent. Usually only the vertical components of the ground motion are considered, because the vertical plane contains the propagation of Rayleigh waves. Through the analysis of the array data, it is possible to retrieve the relation between velocity (or slowness) and frequency, the so-called dispersion curve (hereinafter DC). This curve is related to the structure of the subsoil, so the final step is to search for models of the subsoil that fit the data. As usual in geophysics the solution of this problem, that is called inversion, is not unique: different soil profiles might explain the same data set with an equal misfit. Adding constraints to the inversion should lead to the more realistic class of solutions or soil models.

In our study we applied the 2D passive array techniques in two parts of the MVUB identified by the previous HVNSR analysis. The first experiment is located in the southernmost zone of the basin around the accelerometric station IT.CSA. Considering

the area where the arrays were performed, the obtained velocity profile is reasonably characteristic of the central part of the MVUB.

The second experiment is located in the northern zone of the MVUB. In this area the HVNSR results suggested a possible variation of the subsoil response. In particular, the absence of the resonance peak at about 1 Hz suggests the lack of a velocity contrast in the subsoil and there are two possible reasons for this: i) the absence of the deep layer (Bevagna unit); ii) the Vs increase of the shallow layer (alluvial deposits) close to the Chiascio river that could generate a lower impedance contrast with the Bevagna unit. Therefore, this array was designed with the aim to characterize especially the velocity profile of the shallowest layers (recent alluvial deposits).

#### 4.3.1 Arrays around IT.CSA

The survey consisted of two 2D passive arrays with spiral geometry and different aperture (bottom right zoom in Fig. 3). The small one (150 m aperture, minimum interstation distance of 10 m) consisted of 72 vertical 4.5 Hz geophones connected to a GEODE multichannel acquisition system. With this equipment, both connections among geophones and to the digitizers required cables, then a fully free field area was needed. The uniformity of the geological setting over a large extent, allowed us to find a suitable area 400 m away from station IT.CSA. Moreover, the availability of the manual trigger for starting the acquisition avoided the use of GPS antennas for the synchronization. Overall, ten noise windows, each 8-minutes long, were collected using a sampling rate of 125 sps.

The big array (725 m aperture, minimum interstation distance of 50 m), conversely, was centered around the accelerometric station using 14 stand-alone 3-component velocimetric stations (Reftek R130 digitizers and Lennartz Le3d-5s sensors) synchronized with GPS antennas. The common noise recording lasted about 2 hours.

The minimum and maximum distances of the two arrays were decided with the aim to investigate different but overlapping frequency ranges, in order to sample large depths maintaining good resolution in the very shallow subsurface.

The Geopsy code (http://www.geopsy.org) was used for the analyses.

The first step of the analysis was to calculate the HVNSR curves for each station of the big array, because it has 3-components recordings. Actually, this analysis is preliminary, in order to verify the 1D assumption of the geology setting under the array. Fig. 6a shows the 14 average HVNSR curves over-imposed each other.

The very good agreement among the measurement points in a wide frequency range states the goodness of the 1D assumption. It is worth noting that one of this 3-components station lies in the area of the small array, confirming that the two areas have similar site response and likely similar geological setting.

**Figure 6 – Results of CSA array analysis. a) Summary of HVNSR curves for the 14 stations of big array. Left: plot of the single 14 curves. Right: average and standard deviation values of all; b) Dispersion curves obtained from array analysis at CSA site. Left: small array FK; Center: big array FK. Results are shown with the picking of the dispersion curves and the associated error. The black solid/dotted curves represent the resolution limits of the array for this technique. Right: big array MSPAC. Black solid/dotted curves and grey lines delimit the part of dispersion curve selected for the inversion process.**

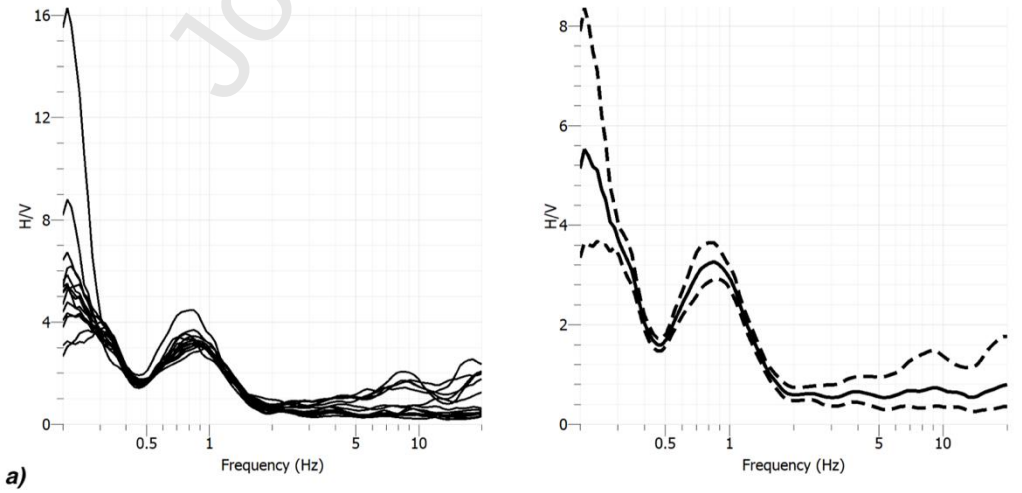


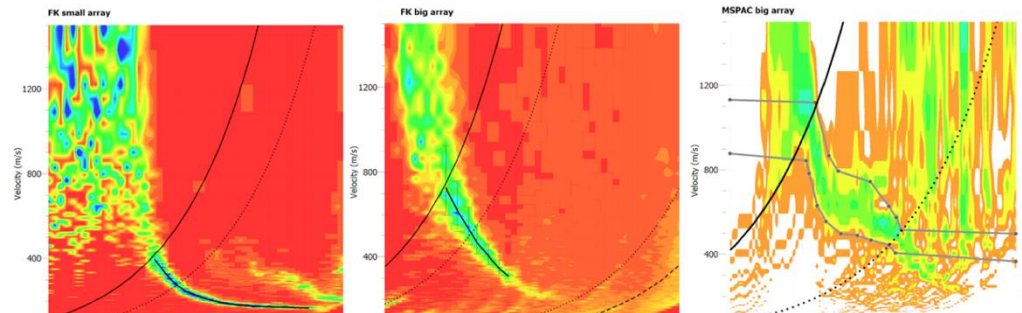

The average HVNSR curve is in agreement with the general results showed previously, with two main peaks at 0.25Hz and 0.85Hz, respectively, that can be attributed to two strong impedance contrasts at depth. Under the hypothesis that the noise wavefield is mostly composed of Rayleigh waves (see Section 4.2), the average HVNSR curve can be interpreted as ellipticity curve.

Data of the two arrays were analyzed independently each other through the conventional beamforming FK method (Lacoss and Kelly, 1969) in order to extract the DC (Fig. 6b).

The big array allowed to reconstruct the DC from 0.8 to 2 Hz whereas the smaller one allowed to infer the DC from 1.5Hz to 10Hz. The two curves overlap fairly well and they were merged to obtain a unique DC.

Although the non-circular shape geometry of the big array, its data can be analyzed also through the modified spatial autocorrelation method (MSPAC) (Bettig et al., 2001). This technique allows an estimation of the frequency-dependent phase velocity from the azimuthal-averaged autocorrelation curves without considering the direction of propagation and number of incoming waves (e.g. Aki 1957, Bonnefoy-Claudet et al., 2008) and finally the determination of the dispersion curves over a wider frequency range with respect to the conventional FK method (e.g. Lacoss and Kelly, 1969, Havenith et al., 2007). Figure 6b (right) shows the dispersion curve retrieved from MSPAC, which is good down to 0.4-0.5 Hz. Figure 3 of Supplementary Materials also shows the autocorrelation curves calculated from the rings each containing a subset of couple of stations ordered by distance and azimuth. The black dots indicate the spatial autocorrelation coefficients providing phase slownesses that contribute at best to the dispersion curve.

The Geopsy code provides the "dinver" tool for the inversion (Wathelet, 2008), that uses a Monte Carlo-like approach, the so-called neighborhood algorithm (Sambridge, 1999), to search for models of the subsoil that fit the data. For constraining the results of the inversion process, we set several targets: the merged dispersion curve, the points of the autocorrelation curves that contribute best to the dispersion curve, and the ellipticity curve. All these targets are given with an associated error. The parametrization used in the inversion, consisted of a three-layer model over half-space, leaving the possibility of large variations in velocity and thickness: the first layer is supposed to have a linear increase in velocity whereas the other two layers are supposed to have a uniform velocity. The Vp values are always linked to the Vs values. The results in terms of a subset of best velocity profiles (Vp and Vs) are shown in Fig. 8 left, while in Figure 4 of Supplementary Materials the fit between experimental targets and forward modeling using the best models is presented. The fit of the autocorrelation curves is almost perfect, whereas the fit of the dispersion curve is very good except for the very low frequency part, even if the result is within the associated standard deviation. A similar behavior is shown for the ellipticity curve: the peak at 0.85 Hz is perfectly reproduced whereas the peak at 0.25 Hz has a larger misfit, even within the associated standard deviation. This issue is not surprising given the decrease in resolution with depth of the array technique. In other words, the interface at 800mt depth and the associated velocity are not completely constrained by our data, nevertheless the obtained values, in particular the depth, are reliable because in agreement with other independent information, such as the seismic

reflection profile performed (Barchi and Lemmi, in press) in the southernmost part of the VUB.

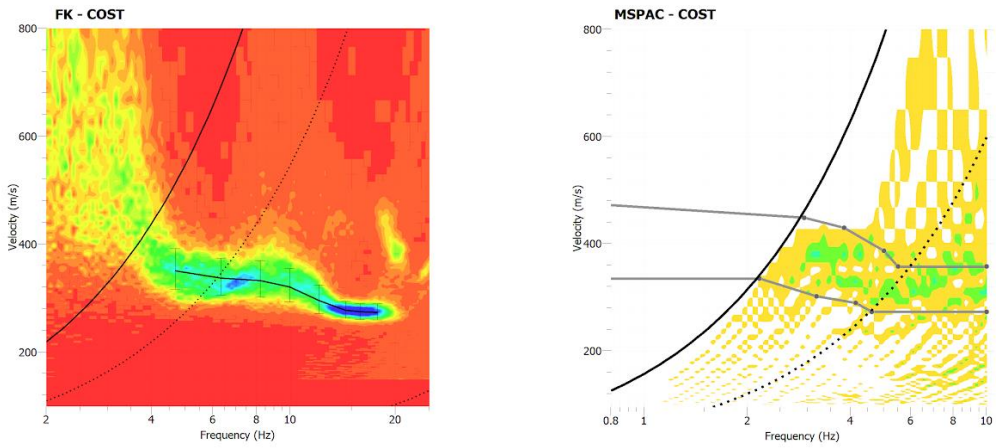


**Figure 7 – Dispersion curves obtained from array analysis at COST site. Left: Plot of FK results with the picking of the dispersion curve (black line) and the associated error. The black solid/dotted curves represent the resolution limits of the array for this technique. Right: Plot of MSPAC results. Black solid/dotted curves and grey lines delimit the part of the dispersion curve selected for the inversion process.**

#### 4.3.2 Array in the northern zone of the MVUB

The survey in the northern zone of the MVUB (hereinafter COST) consisted of a 2D passive array with a spiral geometry and using 24 vertical geophones with corner frequency of 4.5 Hz. One of the geophones was located in the center, whereas the aperture of the array was 48 m and the minimum interstation distance of around 10 m. The recording was similar to what done around IT.CSA, that is ten noise windows, each 8-minutes long, using a sampling rate of 128 sps and an accurate positioning of the geophones through a differential GPS. The central geophone was co-located to a 3-component seismic station with Lennartz 5s velocimeter to acquire ambient noise and get the ellipticity curve from HVNSR data analysis.

FK analysis permitted us to pick the maxima of the dispersion curve in the frequency range between 4.5 and 18 Hz (Fig. 7 left), while the dispersion curve derived from MSPAC analysis, although not well constrained in terms of velocity as the one obtained at CSA site, allowed us to go down to 2.5 Hz (Fig. 7 right). Therefore, it was possible to select some branches of the autocorrelation curves (black portions of the curves in the bottom part of Fig. 5 in Supplementary Materials) to contribute to the inversion process.

We decided to jointly invert the results of FK and MSPAC analysis with the lower part of the ellipticity curve (from 0.2 to 1.5 Hz) containing the resonance peaks to constrain the deepest part of the subsoil down to the geologic bedrock.

Considering the elongation of the valley, the subsoil conditions of the site are expected to be similar to the CSA site. Therefore, for the inversion process the same input model was used. In particular, the starting model is made by 3 layers over half-space, with the shallower layer with a linear increase of the velocity.

The best models obtained from the inversion fit quite well all the imposed targets. As observed for the inversion of the other 2D arrays, the modeled ellipticity curve does not

agree completely with the real fundamental resonance peak. This implies that the obtained velocity model has poor accuracy at higher depths, inducing errors in the estimation of the velocity and thickness of the sedimentary cover over the geological bedrock. The ground profiles obtained from the inversion reflect the starting model, 3 layers over a half-space. The shallow layer presents a linear increase of the velocity from 300 to 470 m/s in the first 40 meters, the second one below has thickness of 40 meters and lower velocity (around 250 m/s), the third layer has a velocity of 750 m/s and reaches 750 m of depth.

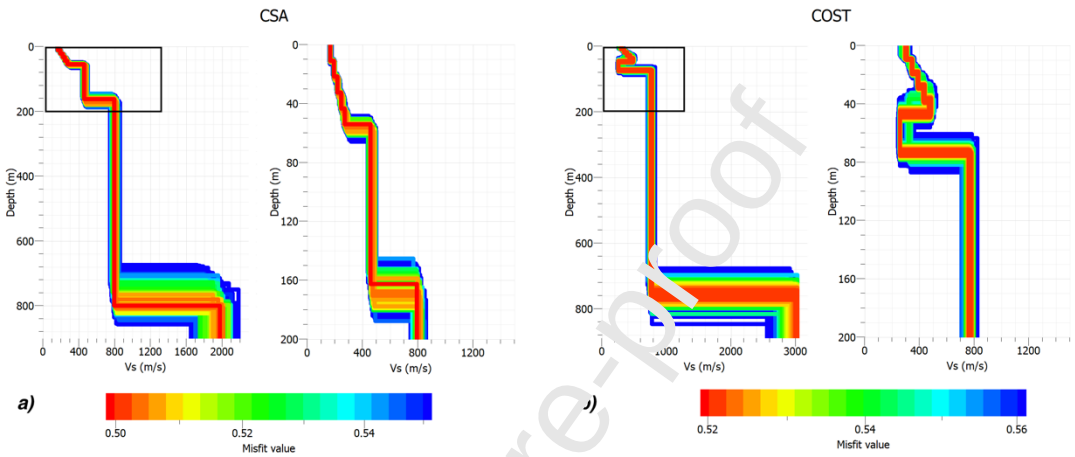


**Figure 8 –Vs profiles obtained from the inversion of array data collected at CSA (a) and COST (b) sites. Left: Complete profiles; Right: zoom of the first 200 m of**

Comparing the subsoil profiles obtained for the two sites (Fig. 8), some differences are visible. If we focus the attention on the shallowest part, Vs is higher for COST site with respect to CSA site. Moreover, the best models obtained from the inversion of COST site reveal the possibility of a velocity inversion just below the shallowest layer in the southern part of the MVUB, which conversely reproduces an increasing velocity of deposits with depth. The striking velocity inversion in Vp profile at around 40 meters for COST site could be due to the fact that no specific velocity conditions has been assigned to Vp input model, except the fact that Vp is constrained to Vs (depending therefore on Vp/Vs value), so that the Vp best fit model needs this kind of artefact to minimize the misfit. Moreover, the higher shear wave velocities of the shallowest layer in the COST site, together with the velocity inversion, could be responsible for the absence of the resonance peak at around 1 Hz, as highlighted by HVNSR results for the northern sites of the study area. As regards the low part of the velocity profiles, the low resonance peak (F0) visible in almost all the HVNSR curves helped in the inversion process to constrain the depth of the deepest impedance contrast. The fundamental resonance peak for almost all the sites investigated is attested between 0.2 and 0.4 Hz and corresponds, for an average velocity of around 800 m/s retrieved from the velocity profile at both CSA and COST sites, at maximum depths of 900m. This velocity contrast is ascribable to the presence of the top of the geological bedrock; the depths of the interface seem quite reasonable but the velocity retrieved should be regarded carefully, given the high uncertainties of the models at those depths.

## 5. Evaluation of the site response through the analyses on earthquakes

The site-to-reference spectral ratio (SSR) technique from earthquake data was first introduced in the '70 as an effective experimental method to retrieve the amplification transfer function for a site. In particular, Borcherdt (1970) used the simultaneous earthquake recordings for a specific site and for a nearby rock site, for which no amplification is expected and can be

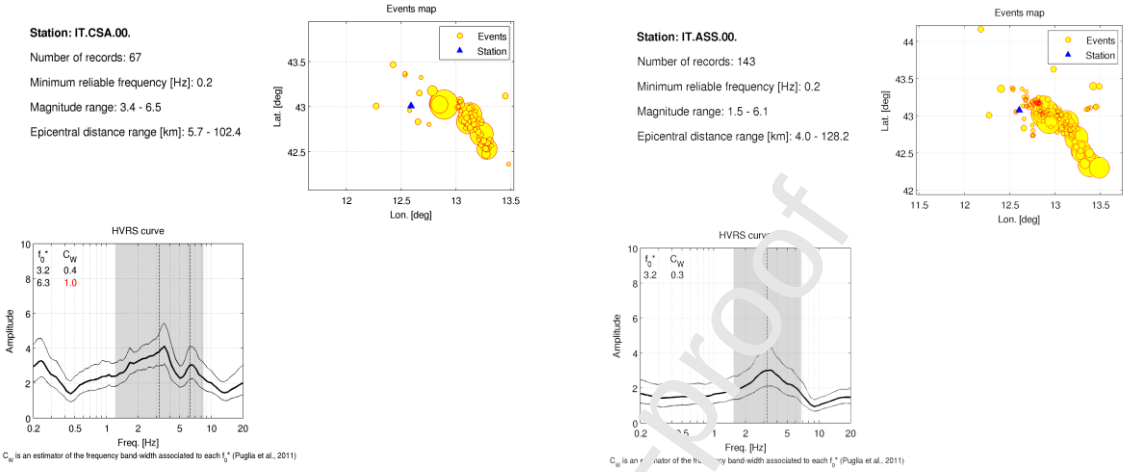


considered as a reference. Considering that the spectrum of an earthquake is influenced by the contribution of the source, the path and the site, averaging results of earthquakes with a good azimuthal cover and a wide magnitude range allows to minimize the influence of the first two parameters, accounting only for the contribution of the site. Assuming that the vertical component of the earthquake recording is not affected by amplification phenomena, Lermo and Chavez-Garcia (1993) replaced the reference site with the vertical component at the given site and calculated the spectral ratios between horizontal and vertical spectra (HVSR). If this assumption is not verified, the HVSR amplification values underestimate the real amplification of the site.

We applied the two spectral ratios techniques (SSR and HVSR) to a selection of earthquake recordings of IT.CSA station. As reference station for the SSR technique we chose the

**Figure 9 - Selection of earthquakes extracted from ITACA database, their location and results of a standard analysis (HVSR) obtained with those data for the two stations considered to put in evidence the response of the site.**

station IT.ASS. While the first one is installed on the soft soils of the MVUB, the second one is installed 7 km away from it, at the Assisi village, which is founded on the limestones of UCS. This site is considered as a Site Class B for EC8 code in the ITACA database (Luzi et al., 2016). However, the database reported also the HVSR analysis, pointing out that this site does not show any amplification site effects between 0.2 to 2 Hz. This frequency range is the most interesting for IT.CSA station, so we decided to consider IT.ASS as a reliable reference site for SSR analysis. Above 2Hz station IT.ASS has some amplification effect that make it not usable for this technique.

We extracted from ITACA database a collection of 43 local earthquakes simultaneously recorded by IT.CSA and IT.ASS stations (in Fig. 9 their location). As general criterion for the

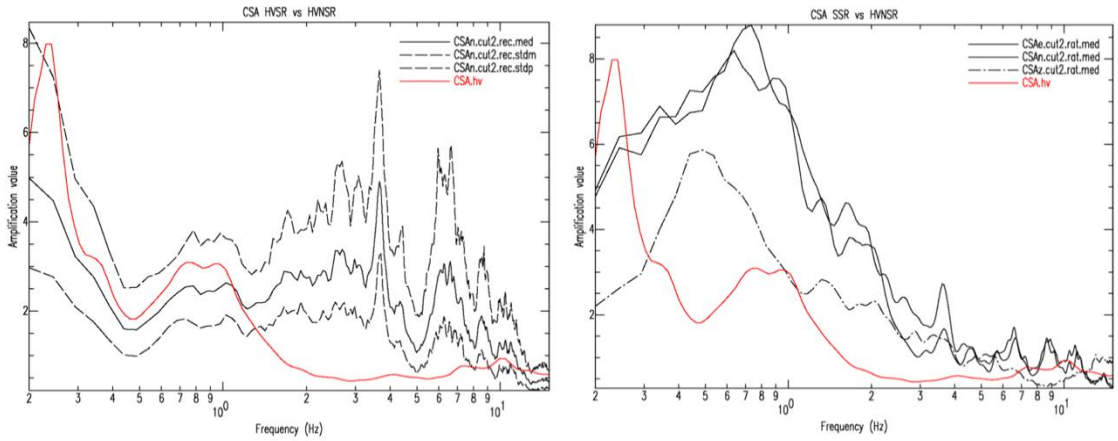


selection, we imposed that the epicentral distance from the two stations was at least 30 km. This constraint assures that the sources of the events are punctual for both stations and the wave-front is approximately to be planar.

The S-waves arrival for each earthquake was manually picked and we considered 20-second long windows for the analyses. The results of both SSR and HVSR analyses are reported in Fig. 10 and compared with HVNSR results.

**Figure 10 - Spectral ratios analysis on a selection of events with maximum epicentral distance of 120 km. Left: comparison between HVSR and HVNSR for CSA site. Right: comparison between the average of the SSR of the 3 components (solid lines for horizontals, dotted line for vertical) and HVNSR for CSA site.**

HVSR results (on the left) highlight the presence of a smooth peak at around 0.8 Hz, as remarked by HVNSR curve (plotted in red). Moreover, HVSR analysis revealed an amplification pattern at higher frequencies that is completely missing in the HVNSR curve. This is a very well-known behavior in literature (e.g. Kawase et al., 2018) and in general is due to the different nature of the wave-field of microtremors and earthquakes.

The SSR results (on the right) were calculated considering the three components. In particular, the dotted curve is the SSR of the vertical component and shows a clear peak at 0.5 Hz. This highlights that also the vertical component is affected by amplification, and it is related to the amplification of the P-wave front propagating through the superficial covers. Comparing vertical SSR (black dotted) and HVNSR (red) curves and assuming a similar relationship between the frequency peaks, the thickness and the velocity of the corresponding type of wave, we can infer the Vp/Vs ratio from the ratio of the main frequency peaks. In this case this ratio is around 2.

SSR of horizontal components reproduce quite well the resonance peak at 0.8 Hz, while they do not show any amplification around the fundamental resonance peak at 0.23 Hz. This is reasonable if we consider the low-resolution in that frequency range due to the shortness of the time windows extracted from the events for the SSR computation. Above 1 Hz some other low amplitude peaks are present, as better highlighted in HVSR curves. As we anticipated in the assumptions, the reliability of the empirical transfer function was limited up to 2 Hz because of the amplifying characteristics of the reference station used for SSR analysis.

The shear-wave velocity model obtained through the results of the 2D arrays at CSA can be used to compute the SH synthetic transfer function and compare it to the empirical transfer function obtained through the SSR analysis. The synthetic transfer function calculation is based on the reflectivity method, as implemented by Bard and Gabriel, (1986), and is made by using the Gpsh module of Geopsy.

From the comparison of the empirical and SH transfer function (Fig. 11) some observations are possible. In terms of resonance peaks, the synthetic curve reproduces quite well the resonance peaks obtained from the SSR analysis in all the frequency range. This reflects that the 1D-response of CSA site is a good assumption. Differences in amplitude are also evident. In the 0.2 - 2Hz, the SSR curve shows higher amplitude values than the SH transfer function. This could be due to the fact that the synthetic transfer function considers only the contribution of a vertical incident S-wave while the SSR curve was computed considering a 20-seconds window to be able to cover the frequency range above 0.2 Hz. Windows with this duration, for the selection of events considered, unavoidably include the contribution of coda waves which give an important energetic contribution in the low frequency range, increasing the SSR amplitude values. Above 2 Hz the SSR curve is not reliable because of the amplification effects occurring at the reference site IT.ASS. Despite that, we can observe a quite good agreement in the frequency of the peaks of the black and red curves, as a demonstration that the velocity model used to reconstruct the SH transfer function is very accurate at shallow depths.

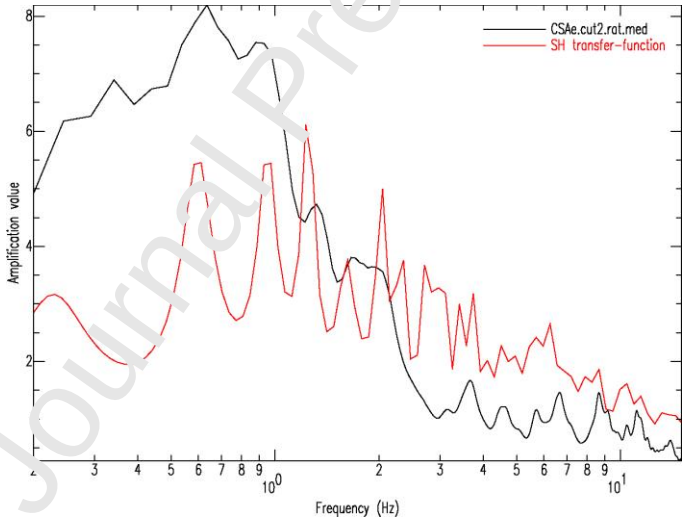


**Figure 11 – SSR (black curve) vs SH transfer function (red curve) at CSA site.**

## 6. Discussion

This is the first study focused on the reconstruction of the buried geological features and the site effects estimation of the MVUB. We applied a multidisciplinary approach, starting from previous knowledge of the surface and subsurface geology to plan the single station microtremor and passive array campaign and interpret results obtained to improve the details of a subsurface geological model, extended down to a depth of about 1000 m.

HVNSR curves were represented as contour plots along the two studied transects (Fig. 4, bottom), representing the first important result which effectively illustrates both vertical and

horizontal variability within the basin succession and offering the possibility of a prompt geological interpretation. In general, along the longitudinal (NW-SE) transect the main impedance contrasts are laterally continuous, as expected in the direction parallel to the basin axis, which is also parallel to the maximum elongation and continuity of the geological bodies. However, the highest frequency peak (at about 1 Hz) clearly diminishes its amplitude in the northern part: this can be explained with the presence, within the shallow stratigraphic layer, of the alluvial fan of the Chiascio river, whose coarse sediments (mostly carbonate gravels) offer a lower impedance contrast with the underlying, older lacustrine succession (TLS). The transversal (SW-NE) transect, in turn, shows a much larger lateral variability, highlighting the main structural features controlling the onset and evolution of the basins. Along this transect, the sudden and significant increase of the peak amplitudes in the central part of the basin corresponds to the portion characterized by the larger thickness of the sedimentary sequence, whilst the SW and NE limits of this region mark the position of the buried major, opposite-dipping normal faults, bordering the basin.

The shallow (about 1 Hz) peak is much more evident in the SW rank respect to the NE one: in the latter, the shallower, alluvial layer mostly consists of coarser sediments, derived from the debris flows coming from the M. Subasio carbonate anticline. The stratigraphy of the axial (i.e. deeper) part of the basin and the mechanical characteristics of the main layers have been further investigated through two arrays, located at CSA and COST site respectively, producing 1-D velocity models, extended down to the geological bedrock, at an estimated depth of about 800 m (Fig. 12). The 1-D Vs profile at the CSA site, generally representative of the syn-tectonic succession infilling the axial part of the MVUB, includes three layers. In the shallowest layer, about 55 m thick, Vs gradually increases up to a value of about 300 m/s, the intermediate layer shows a constant value of about 450 m/s, and its bottom is located at a depth of about 160 m. These two layers are here interpreted to correspond to the recent (i.e. Late Pleistocene-Holocene) alluvial sediments infilling the MVUB present-day plain. The much thicker deep layer, reaching a depth of about 800 m, is characterized by a Vs of about 800 m/s, and is interpreted to correspond to the Early Pleistocene, well-consolidated fluvio-lacustrine succession of the "Tiberino Basin" (e.g. Bizzarri et al., 2018; Bevagna Unit, e.g. Barchi and Lemmi, in press). The velocity profile retrieved at the CSA station, located in the central part of the basin, allowed to convert to depth the frequency of the F1 peak, showing a good fit between geophysical and geological data. This is possible by using a simplified evaluation (quarter wavelength formula, e.g. Joyner et al. 1981, Poggi et al., 2012) which correlates the frequency of the resonance peak with the thickness of the layers and their average shear wave velocity. For an average Vs of 250 m/s (Fig. 8 for the velocity profile), F1 peaks correspond to depths between 30 and 75 m below the surface. HVNSR curves do not show any resonance peak at frequencies compatible with the depth of the interface between the deep gravels and sands (alluvial) deposits and the Bevagna Unit (TLS). This could be related to the over-consolidation of TLS at those depths, as reported in the description of the stratigraphic profiles, which could give Vs values close to the overlaying alluvial deposits. To check this hypothesis, we compare the two velocity profiles retrieved for CSA and COST sites. The COST site, located 6 km to the NW, is representative of a peculiar situation, related to the presence of the coarser sediments of the Chiascio alluvial fan, with a relatively high Vs (increasing up to a value of 470 m/s at a depth of about 40 m), overlying a low-velocity (Vs = 250 m/s) layer of fine-grained sediments, down to a depth of 80 m. The underlying layer, with a Vs of 750 m/s, extends down to a depth of 750 m, including the lower part of the recent alluvial deposits and the underlying Early Pleistocene TLS (Bizzarri et al., 2018).

The results of the geophysical survey, described in this paper, integrated by previous geological and geophysical knowledge, are synthetized in the schematic geological cross-

section of Fig. 12, where the subsurface structure of the basin is illustrated, along with the position and geometry of the major faults, which are thought to control the basin onset and evolution.

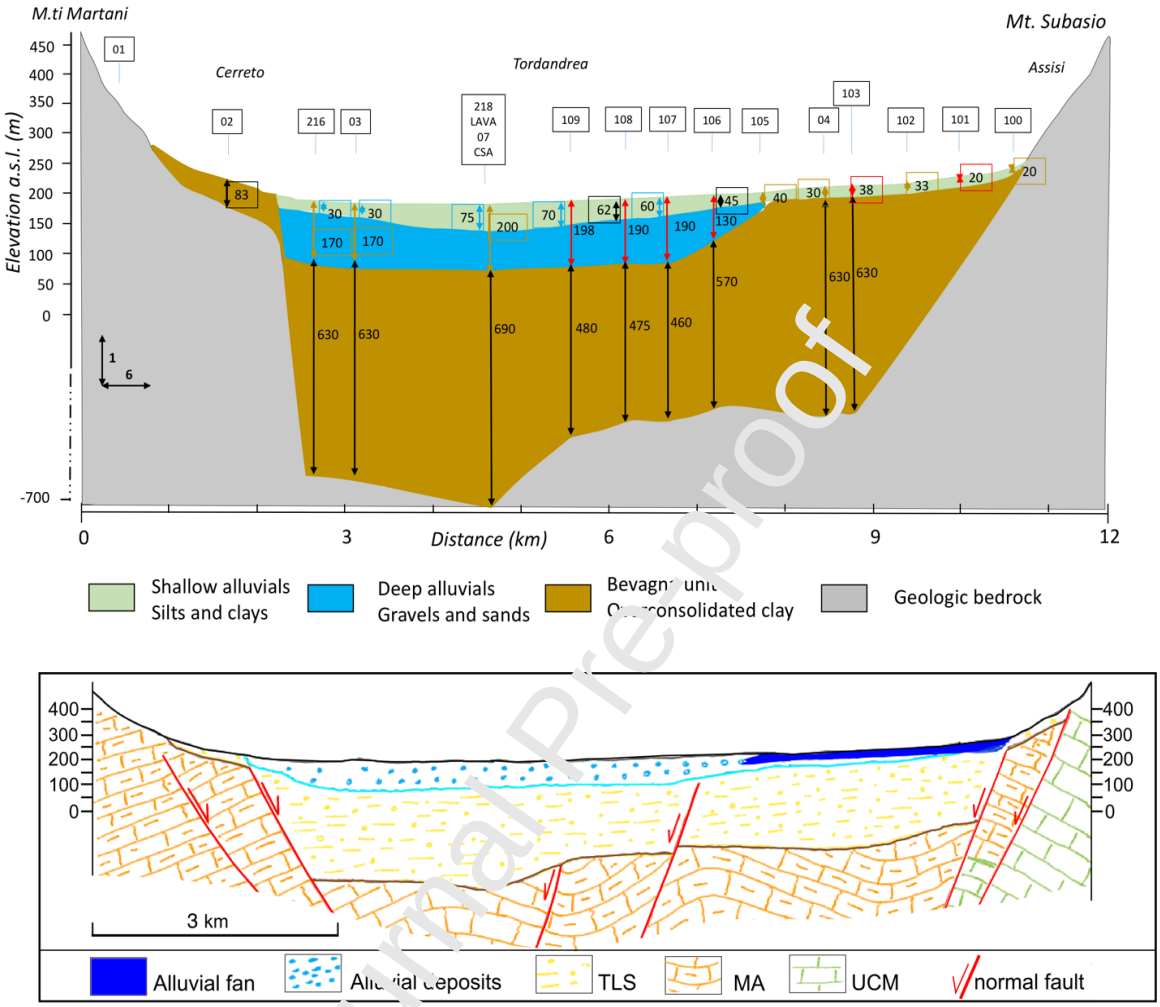


**Figure 12 - Top: Geological reconstruction of MVUB along a SW-NE transect by using geological (brown and blue arrows) and geophysical (black arrows) constrains. Red labels are inferred values. The vertical scale is exaggerated 6 times. Bottom: Geological section realized considering the tectonic setting and the morphological features of the area. The vertical scale in exaggerated 3 times.**

The section shows the MVUB as a graben, controlled by two sets of opposite dipping (i.e. NE and SW-dipping) normal faults. At the two flanks of the MVUB, a different geological bedrock crops out, consisting of Miocene turbidites (Marnoso-Arenacea Fm.) in the SW flank and of older Mesozoic-Paleogene carbonates (UCS) in the NE flank, corresponding to the large anticline of M. Subasio. However, along the NE flank, the MA turbidites crop out in an intermediate fault block, suggesting that the central part of the basin is also floored by deformed Miocene turbidites, unconformably overlaid by the lacustrine succession TLS. In this central part, our survey indicates that the total thickness of the sedimentary succession is in the order of 800 m, a value which is consistent with previous studies, mostly based on seismic reflection survey (Barchi et al., 1991; Barchi and Lemmi, in press) or on geo-electrical prospections (AA.VV., 1991). It is worth to mention that since the study area is a quaternary tectonic valley, 2D/3D site effects could affect the site response. In fact, H/V

peaks obtained for almost all the sites fit quite well the 1D response of the area and in particular: the higher frequency peak matches very well the geological evidence available for the area (borehole data), while the lower frequency one is supported by the seismic reflection profile previously performed in the southern part of the VUB which gives an idea of the trend of the geological bedrock and the average thickness of the filling. Despite this, further investigations and data analysis will be performed to better detail the sites with possible evidences of 2D/3D effects such as the basin edges and fault zones.

The relevant thickness (about 150 m) of the recent alluvial sediments indicates a relatively high subsidence rate of the hanging-wall block suggesting that the basin-bounding faults are capable to counteract for the regional uplift. In addition, the presence of significant historical and instrumental seismicity, point to the conclusion that these faults are still active and responsible of the seismic activity of the area.

Results from earthquake recordings at CSA Italian accelerometric station and standard spectral ratios techniques (HVSR and SSR) lead to the following conclusions: the amplification of the central part of the basin reaches values higher than 5 for frequencies below 1 Hz. SSR also gives clues about the Vp/Vs ratio for the area which results to be around 2. Average Vp and Vs values derived from the quarter wavelength formula applied on SSR and HVNSR fundamental resonance peaks are 1800 m/s and 900 m/s respectively. From the comparison of the synthetic SH-transfer function calculated for CSA site and the SSR curve it is possible to observe a similar trend between the resonance peaks modeled and the empirical ones. SSR curve is reliable below 2 Hz (as already considered in our initial hypotheses) and its amplitude values are higher than the ones modeled because, for the computation, we had to select a 20s-window of each event which also included coda waves. This caused an increase of the energy involved for frequencies below 1 Hz.

## 7. Conclusions

Two main multidisciplinary geophysical techniques were applied in this study. Combining single station ambient noise measurements and passive array techniques we were able to reconstruct the general trend of the hidden geometries of the study area and associate a geological interpretation to them.
The velocity profiles derived from array analysis at CSA and COST sites were used to convert the resonance frequency of single station measurements into depth for sites with a similar stratigraphic setting. To give a geological meaning to all the geophysical results obtained, we reconstructed a SW-NE geological section for which the trend of the subsurface geometries is mainly driven by the match of HVNSR results, velocity profiles and geological constraints as borehole logs and outcropping geology.

Analysis of earthquakes and 1D numerical simulations led us to the estimation of the amplification function for the central part of MVUB, verifying that the synthetic and the empirical transfer functions show a good agreement of the resonance peaks especially in terms of frequency. The results of this work represent a good starting point to improve the knowledge of the subsurface of the area in terms of geological features which play an important role for the seismic risk evaluation of MVUB. As a matter of fact, the widespread geophysical campaign performed gives clues about the parts of MVUB more prone to amplification effects due to seismic shaking. The proposed geological model puts in evidence the presence of active faults within the MVUB that should be investigated more in detail with

classical techniques such as seismic reflection profiles, vertical electrical tomography and, in some cases, also paleo-seismological trenches to reveal their historical activity and improve the hazard assessment of central Italy.

This study clearly demonstrates that the ambient noise measurement revealed to be an effective, relatively quick and low-cost geophysical technique, for the detection of the stratigraphic and structural subsurface setting of the study area. Our feeling is that this technique can be successfully applied to other basins in similar geological environments, i.e. continental basins infilled by clastic sedimentary successions, less than 1 km thick.
In particular, the proposed approach could be easily extended to the continental intramountain basins of the Apennines, as a fast, relatively low-cost survey of thickness and lithological characterization of their infilling sedimentary successions. Since the evolution of these basins is strictly associated to the relevant seismicity of the Apennines ridge, a better knowledge of their geometry and thickness can contribute to clarify the regional seismo-tectonic scenario.

The relevant results of this study might be possibly further improved by acquiring at least one high-resolution seismic reflection profile across the basin, which could better quantify the slip on each fault and define more clearly the depths of the geologic bedrock adding more constrains to the model proposed in this study.

**Acknowledgements**

This study benefitted from array data collected in the framework of task 4 DPC-INGV B2 project for the characterization of Italian accelerometric station IT.CSA therefore we thank all the participants to the geophysical campaign who helped to perform array measurements. We also thank Giuliano Milana for the fruitful discussions. We are grateful to Lorena Fastellini (owner of "Il Lavandeto di Assisi") and l'Hazienda which made our field activities easier and more enjoyable thanks to their availability and kindness.

**References**

Aki, K. (1957), Space and time spectra of stationary waves with special reference to microtremors, Bull. Earthquake Res. Inst. Univ. Tokyo, 35, 415–456.

AA.VV. (1991). Le acque sotterranee in Umbria (The groundwater in Umbria). A cura di S. Giaquinto, G. Marchetti, A. Martinelli, E. Martini, 212 pp., Protagon -GNDCI-CNR (pubbl. 413), Perugia.

Albani, A. (1962). L'antico lago tiberino. Istituto geografico militare.

Ambrosetti, P. (1982). Il sollevamento dell'Italia centrale tra il Pleistocene inferiore e il Pleistocene medio. Contributi conclusivi per la realizzazione della carta neotettonica d'Italia. PF Geodinamica-CNR, 513, 219-223.

Ambrosetti, P., Basilici, G., Capasso Barbato, L., Carboni, M. G., Di Stefano, G., Esu, D., Gliozzi, E., Petronio, C., Sardella, R. & Squazzini, E. (1995). Il Pleistocene inferiore nel ramo Sud-Occidentale del Bacino Tiberino (Umbria): aspetti litostratigrafici e biostratigrafici. Il Quaternario, 8(1), 19-36.

Ambrosetti, P., Carboni, M. G., Conti, M. A., Esu, D., Girotti, O., La Monica, G.B., Landini, B. & Parisi, G. (1987). Il Pliocene ed il Pleistocene inferiore del bacino del Fiume Tevere nell'Umbria meridionale. Geografia Fisica e Dinamica Quaternaria, 10(1), 10-33.

Anderlini, L., Serpelloni, E., and Belardinelli, M.E. (2016). Creep and locking of a low-angle normal fault: Insights from the Altotiberina fault in the Northern Apennines (Italy): Geophysical Research Letters, v. 43, p. 4321–4329, doi:10.1002/ 2016GL068604.

Argenti, P. (2004). Plio-quaternary mammal fossiliferous sites of Umbria (Central Italy). Geologica Romana, 37(2003-2004), 67-78.

Barchi, M.R. (2010). The Neogene-Quaternary evolution of the Northern Apennines: crustal structure, style of deformation and seismicity, in Beltrando, M., Peccerillo, A., Mattei, M., Conticelli, S., and Doglioni, C., eds., The Geology of Italy: Journal of the Virtual Explorer, Electronic Edition, ISSN 1441-8142, v. 36, paper 10, doi: 10.3809/jvirtex.2010.00220.

Barchi, M.R., Lemmi M. a cura di (in press) - Note illustrative della Carta Geologia d'Italia, scala 1:50,000 - Foglio 324 - Foligno.

Barchi, M., Brozzetti, F., Lavecchia, G. (1991). Analisi strutturale e geometrica dei bacini della media valle del Tevere e della valle umbra. Bollettino della Società Geologica Italiana, 110(1), 65-76.

Barchi, M., and M. Ciaccio (2009). Seismic images of an extensional basin, generated at the hanging-wall of a low-angle normal fault: The case of the Sansepolcro basin (central Italy), Tectonophysics, 479, 285–293.

Barchi, M.R., Minelli, G. and G. Pialli (1998). The CROP 03 profile: A synthesis of results on deep structures of the northern Apennines, Mem. Soc. Geol. Ital. 52, 383–400.

Barchi, M., and F. Mirabella (2009). The 1997–98 Umbria-Marche earthquake sequence: Geological vs. seismological faults, Tectonophysics, 476, 170–179.

Bard, P.Y. and J.C. Gabriel (1986). The seismic response of two-dimensional sedimentary deposits with large vertical velocity gradients, Bulletin of The Seismological Society of America, Vol. 76, pp. 343-366.

Barker, G. (1984) Ambiente e società nella preistoria dell'Italia centrale - NIS, La Nuova Italia Scientifica, Studi NIS Archeologia 2, Arti Grafiche Editoriali S.r.l. Urbino, pp. 262.

Basili, R., G. Valensise, P. Vannoli, U. Fracassi, S. Mariano, M. Tiberti, and E. Boschi (2008). The Database of Individual Seismogenic Sources (DISS), version 3: Summarizing 20 years of research on Italy's earthquake geology, Tectonophysics 453, 20–43.

Basilici, G. (1997). Sedimentary facies in an extensional and deep-lacustrine depositional system: the Pliocene Tiberino Basin, Central Italy. Sedimentary Geology, 109(1-2), 73-94.

Beretta, G.P., Avanzini, M., Marangoni, T., Burini, M., Schirò, G., Terrenghi, J., Vacca, G. (2018). Groundwater modeling of the withdrawal sustainability of Cannara artesian aquifer (Umbria, Italy). Acque Sotterranee-Italian Journal of Groundwater, 7(3), 47-60.

Bettig, B., Bard, P.Y., Scherbaum, F., Riepl, J., Cotton, F., Cornou, C., Hatzfeld, D. (2001). Analysis of dense array noise measurements using the modified spatial auto-correlation method (SPAC): application to the Grenoble area, Boll. Geof. Teorica Appl. 42, nos. 3–4, 281–304.

Bizzarri, R., Albianelli, A., Argenti, P., Baldanza, A., Colacicchi, R., Napoleone, G. (2011). The latest continental filling of Valle Umbra (Tiber Basin, central Italy) dated to one million years ago by magnetostratigraphy. Il Quaternario, 24(1), 51-65.

Bizzarri, R., Corrado, P., Magri, D., Martinetto, E., Esu, D., Caprai, V., ... & Baldanza, A. (2018). Palaeoenvironmental and climatic inferences from the late early Pleistocene lacustrine deposits in the eastern Tiberino Basin (central Italy). Quaternary Research, 90(1), 201-221.

Boncio, P., G. Lavecchia, and B. Pace (2004) Defining a model of 3D seismogenic sources for seismic hazard assessment applications: The case of central Apennines (Italy), J. Seismol. 8, 408–425.

Bonnefoy-Claudet, S., Cornou, C., Bard, P.-Y., Cotton, F., Moczo, P., Kristek, J. and Fäh, D. (2006) "H/V ratio: a tool for site effects evaluation. Results from 1-D noise simulations," Geophysics Journal International, 167, 827–837, doi: 10.1111/j.1365-246X.2006.03154.x.

Bonnefoy-Claudet, S., F. Cotton, Bard, P.-Y. (2006). The nature of the seismic noise wave field and its implication for site effects studies: a literature review, Earth Sci. Rev. 79, nos. 3–4, 205–227.

Bonnefoy-Claudet, S. Köhler, A., Cornou, C., Wathelet, M., Bard, P.-Y. (2008). Effects of Love Waves on Microtremor H/V Ratio. Bulletin of the Seismological Society of America, 98(1), 288-300. https://doi.org/10.1785/0120070063.

Borcherdt, R.D. (1970). Effects of local geology on ground motion near San Francisco Bay. Bulletin of the Seismological Society of America, 60(1), 29-61.

Brunori, C.A., Famiani, D., Sapia, V., Villani, F., Pizzimenti, L., Caciagli, M., Melelli, L., Mirabella, F., Barchi, M., (2018). Seismotectonics study of the Media Valle Umbra area at different space and time scales: an integration of geomorphological, geophysical and remote sensing data. The 36th General Assembly of the European Seismological Commission ESC2018-S13-583 doi:10.13140/RG.2.2.13946.95685.

Bucci, F., Mirabella, F., Santangelo, M., Cardinali, M., Guzzetti, F. (2016). Photo-geology of the Montefalco Quaternary Basin, Umbria, Central Italy. Journal of Maps, 12(sup1), 314-322.

Caciagli, M., Pucci, S., Batlló, J., Cesca, S., Braun, T. (2019). Did the Deadly 1917 Monterchi Earthquake Occur on the Low□Angle Alto Tiberina (Central Italy) Normal Fault?. Seismological Research Letters doi: https://doi.org/10.1785/0220180155.

Cattuto, C., Gregori, L., Melelli, L., Taramelli, A., Broso, D. (2005). I conoidi nell'evoluzione delle conche intermontane umbre. Geografia Fisica e Dinamica del Quaternario, 7, 89-95.

Cinque, A., Patacca, E., Scandone, P., Tozzi, M. (1993). Quaternary kinematic evolution of the Southern Appennines. Relationships between surface geological features and deep lithospheric structures. Annals of Geophysics, 36(2).

Cinti, F.R., Alfonsi, L., D'Alessio, A., Marino, S., Brunori, C.A. (2015). Faulting and ancient earthquakes at Sybaris archaeological site, Ionian Calabria, Southern Italy. Seismological Research Letters, 86 (1). doi: 10.1785/02201401071.

Coltorti, M., and Pieruccini, P. (1997). Middle-Upper Pliocene "Compression" and Middle Pleistocene "Extension" in the east Tiber Basin: from "synform" to "extensional" basins in the Tyrrhenian side of the Northern Apennines (Central Italy). Il Quaternario, 10(2), 521-528.

Conti, M.A. and Girotti, O. (1977). Il Villafranchiano nel "Lago Tiberino", ramo sud-occidentale: schema stratigrafico e tettonico. Geologica Romana, 16, 67-80.

Cresta, S., Monechi, S., Parisi, G., Baldanza, A., Reale, V. (1989). Stratigrafia del Mesozoico e Cenozoico nell'area umbro-marchigiana: itinerari geologici sull'Appennino umbro-marchigiano (italia). Istituto poligrafico e zecca dello stato.

D'Agostino, N., Giuliani, R., Mattone, M., Bonci, L. (2001). Active crustal extension in the central Apennines (Italy) inferred from GPS measurements in the interval 1994–1999. Geophysical Research Letters, 28(10), 2121-2124.

D'Agostino, N., Mantenuto, S., D'Anastasio, E., Giuliani, R., Mattone, M., Calcaterra, S., Gambino, P., Bonci, L. (2011). Evidence for localized active extension in the central Apennines (Italy) from global positioning system observations: Geology, v. 39, p. 291-294, doi: 10.1130/G31796.1.

Devoti, R., D'Agostino, N. Serpelloni, E., Pierantonio, G., Riguzzi, F., Avallone, A. & Franco, L. (2017). A combined velocity field of the Mediterranean region: Annals of Geophysics, v. 60, doi:10.4401/ag-7059.

DISS Working Group (2018). Database of Individual Seismogenic Sources (DISS), Version 3.2.1: A compilation of potential sources for earthquakes larger than M 5.5 in Italy and surrounding areas.http://diss.rm.ingv.it/diss/, Istituto Nazionale di Geofisica e Vulcanologia; DOI:10.6092/INGV.IT-DISS3.2.1.

Fäh D. Kind F., Giardini D (2001). A theoretical investigation of average H/V ratios. Geophys. J. Int., 145, 535– 549.

A computer code for forward calculation and inversion of the H/V spectral ratio under the diffuse field assumption. Computer & Geosciences 97, 67-78.

García-Jerez A., Piña-Flores J., Sánchez-Sesma F.J., Luzón F., Perton M. (2016). A computer code for forward calculation and inversion of the H/V spectral ratio under the diffuse field assumption. Computer & Geosciences 97, 67-78. http://dx.doi.org/10.1016/j.cageo.2016.06.016.

Ge.Mi.Na (1962) - Ligniti e torbe dell'Italia continentale: indagini geominerarie effettuate nel periodo 1958-1961 dalla Geomineraria nazionale (GEMINA) di Roma / [a cura della GEMINA]. - Roma: GEMINA, c1962. - 319 p.

Giaquinto, S., and Martinelli, A. (1991). Studi sull'acquifero artesiano di Cannara (Study on the Cannara artesian aquifer). In AA.VV., Le acque sotterranee in Umbria, a cura di S. Giaquinto, G. Marchetti, A. Martinelli, E. Martini, Protagon -GNDCI-CNR (pubbl. 413), 145-167 pp.. Perugia.

Gregori, L. (1988). Il" Bacino di Bastardo"; genesis ed evoluzione nel quadro della tettonica recente. Bollettino della Societá Geologica Italiana, 107(1), 141-151.

Guidoboni, E., Ferrari, G., Mariotti, D., Comastri, A., Tarabusi, G., Sgattoni, G., Valensise, G. (2018). CFTI5Med, catalogue of strong earthquakes in Italy (461 B.C.–1997) and Mediterranean area (760 B.C.–1500), Technical Report, Istituto Nazionale di Geofisica e Vulcanologia, available at http://storing.ingv.it/cfti/cfti5 (last accessed April 2019).

Guzzetti F., Manunta M., Ardizzone F., Pepe A., Cardinali M., Zeni G., Reickenbach P., Lanari R. (2009). Analysis of ground deformation detected using the SBAS-DInSAR technique in Umbria, Central Italy. Pure appl. geoph. 166 (2009) 1425–1459, 0033–4553/09/081425–35, doi: 10.1007/s00024-009-0491-4.

Havenith, H.B., Fah, D., Polom, U., Roulle, A. (2007). S-wave velocity measurements applied to the seismic microzonation of Basel, Upper Rhine Graben. Geoph. J. Int., 170(1), pp 346-358, doi: 10.1111/j.1365-246X.2007.03422.x.

Joyner, W. B., Warrick, R. E., and Fumal, T. E. (1981). The effect of Quaternary alluvium on strong ground motion in the Coyote Lake, California, earthquake of 1979. Bulletin of the Seismological Society of America, 71(4):1333–1349.

Kawase, H., Matsushima, S., Satoh, T., Sánchez-Sesma, F.J. (2015). Applicability of Theoretical Horizontal-to-Vertical Ratio of Microtremors Based on the Diffuse Field Concept to Previously Observed Data. Bulletin of the Seismological Society of America, 105 (6), 3092-3103. https://doi.org/10.1785/0120150134.

Kawase, H., Mori, Y., Nagashima, F. (2018). Difference of horizontal-to-vertical spectral ratios observed earthquakes and microtremors and its application to S-wave velocity inversion based on the diffuse field concept. Earth, Planets and Space, 70:1. https://doi.org/10.1186/s40623-017-0766-4.

Lachet, C. & Bard, P.-Y., 1994. Numerical and Theoretical Investigations on the possibilities and limitations of Nakamura's technique, J. Phys. Earth, 42, 377–397.

Lacoss, R.T., Kelly, E.J. & Toksoz, M.N. (1969). Estimation of seismic noise structure using arrays. Geophysics, 34: 21-38.

Lavecchia, G., Brozzetti, F., Barchi, M., Keller, J., Menichetti, M. (1994). Seismotectonic zoning in east-central Italy deduced from the analysis of the Neogene to present deformations and related stress fields, Geol. Soc. Am. Bull. 106, 1107–1120.

Lermo, J. & Chavez-Garcia, F.J. (1993). Site effect evaluation using spectral ratios with only one station. Bull. Seismol. Soc. Am. 83(5), 1574–1594.

Lermo, J. & Chavez-Garcia, F.J. (1994). Are microtremors useful in site response evaluation? Bull. Seismol. Soc. Am. 84 (5): 1350-1364.

Lontsi, A.M., García-Jerez, A., Molina-Villegas, J.C., Sánchez-Sesma, F.J., Molkenthin, C., Ohrnberger, M., Krüger, F., Wang, R., Fäh, D. A generalized theory for full microtremor horizontal-to-vertical [H/V(z, f)] spectral ratio interpretation in offshore and onshore environments. Geophys. J. Int., 218(2): 1276-1297., https://doi.org/10.1093/gji/ggz223.

Luzi, L., Pacor, F., Puglia, R. (2016). Italian Accelerometric Archive v 2.1. Istituto Nazionale di Geofisica e Vulcanologia, Dipartimento della Protezione Civile Nazionale. doi: 10.13127/ITACA/2.1 (last access May 2019).

Malinverno, A. and Ryan, W.B. (1986). Extension in the Tyrrhenian Sea and shortening in the Apennines as result of arc migration driven by sinking of the lithosphere. Tectonics, 5(2), 227-245.

Mariani, S., Mainiero, M., Barchi, M., Van Der Borg, K., Vonhof, H., Montanari, A. (2007). Use of speleologic data to evaluate Holocene uplifting and tilting: an example from the Frasassi anticline (northeastern Apennines, Italy). Earth and Planetary Science Letters, 257(1-2), 313-328.

Martinetto, E., Bertini, A., Basilici, G., Baldanza, A., Bizzarri, R., Cherin, M., ... & Pontini, M.R. (2014). The plant record of the Dunarobba and Pietrafitta sites in the Plio-Pleistocene palaeoenvironmental context of central Italy. Alpine and Mediterranean Quaternary, 27(1), 29-72.

Martini, I.P., Sagri, M. (1993). Tectono-sedimentary characteristics of Late Miocene-Quaternary extensional basins of the Northern Apennines, Italy. Earth-Science Reviews, 34(3), 197-233.

Melelli, L., Pucci, S., Saccucci, L., Mirabella, F., Pazzaglia, F., Barchi, M. (2014). Morphotectonics of the Upper Tiber Valley (Northern Apennines, Italy) through quantitative analysis of drainage and landforms. Rendiconti Lincei, 25(2), 129-138.

Miller, G. F. & Pursey, H., 1955. On the partition of energy between elastic waves in a semi-infinite solid. Proceedings of the Royal Society of London A: Mathematical, Physical and Engineering Sciences, 233(1192), 55–69.

Mirabella, F., Bucci, F., Santangelo, M., Cardinali, M., Caielli, G., De Franco, R., Guzzetti, F. & Barchi, M. R. (2018). Alluvial fan shifts and stream captures driven by extensional tectonics in central Italy. Journal of the Geological Society, 175(5), 788-805.

Murgia F., Bignami C., Brunori C.A., Tolomei C., Pizzimenti L. (2019) Ground Deformations Controlled by Hidden Faults: Multi-Frequency and Multitemporal InSAR Techniques for Urban Hazard Monitoring. Remote Sens. 2019, 11, 2246; doi:10.3390/rs11192246.

Nakamura, Y. (1989). A method for dynamic characteristics estimation of subsurface using microtremor on the ground surface, Q. Rep. Railway Tech. Res. Inst. 30, no. 1, 25–33.

Nogoshi, M., and T. Igarashi (1971). On the amplitude characteristic of microtremor (part 2) (in Japanese with English abstract), J. Seism. Soc. Japan 24, 26–40.

Petronio, C., Argenti, P., Caloi, L., Esu, D., Girotti, O., Sardella, R. (2002). Updating Villafranchian mollusc and mammal faunas of Umbria and Latium (Central Italy). Geologica Romana, 36(2000-2002), 369-387.

Poggi, V., Edwards, B. and Fäh, D (2012). The quarter wavelength average velocity: a review of some past and recent application developments. 15th WCEE, Lisbon 2012..

Pondrelli, S., Salimbeni, S., Ekström, G., Morelli, A., Gasperini, P., and Vannucci, G., (2006). The Italian CMT dataset from 1977 to the present: Physics of the Earth and Planetary Interiors, v. 159, p. 286-303, doi: 10.1016/j.pepi.2006.07.008,159/3-4.

Pucci, S., Mirabella, F., Pazzaglia, F., Barchi, M. R., Melelli, L., Tuccimei, P., Soligo, M., and Saccucci, L. (2014) Interaction between regional and local tectonic forcing along a complex Quaternary extensional basin: Upper Tiber Valley, Northern Apennines, Italy: Quaternary Science Reviews, v. 102, p. 111-132.

Radmilli, A.M. (1960). Considerazioni sul Mesolitico italiano, "Annali dell'Università di Ferrara" Sez. 15, 1, 29-48.

Ricci Lucchi, F. (1986). The foreland basin system of the northern apennines and related clastic wedges: a preliminary outline: Giornale di Geologia, v. 48, p. 165–185.

Rovida, A., Locati M., Camassi R., Lolli B., Gasperini P., eds., (2016). CPTI15, the 2015 Version of the Parametric Catalogue of Italian Earthquakes: Istituto Nazionale di Geofisica e Vulcanologia. doi: 10.6092/INGV.IT CPTI15.

Saccucci, L. (2011). Analisi geologica e geomorfologica finalizzata alla ricostruzione dell'evoluzione Quaternaria del Bacini Tiberino. PhD Tesi, Perugia University.

Sambridge, M. (1999). Geophysical inversion with a neighbourhood algorithm I. Searching a parameter space, J. Geophys. Res. 103, 4839–4878.

Sánchez-Sesma, F. J., M. Rodríguez, U. Iturrarán-Viveros, F. Luzón, M. Campillo, L. Margerin, A. García-Jerez, M. Suarez, M. A. Santoyo, Rodríguez-Castellanos, A. (2011). A theory for microtremor H/V spectral ratio: Application for a layered medium, Geophys. J. Int. Exp. Lett. 186, no. 1, 221–225, doi: 10.1111/j.1365-246X.2011.05064.x.

Tarquini S., Isola, I., Favalli, M., Mazzarini, F., Bisson, M., Pareschi, M.T., Boschi, E. (2007). TINITALY/01: a new Triangular Irregular Network of Italy, Annals of Geophysics, 50, 407-425.

Wathelet, M. (2008). An improved neighborhood algorithm: parameter conditions and dynamic scaling. Geophysical Research Letters, 35, L09301, doi:10.1029/2008GL033256.

Yamanaka, H., M. Takemura, H. Ishida, and M. Niwa (1994). Characteristics of long-period microtremors and their applicability in exploration of deep sedimentary layers, Bull. Seism. Soc. Am. 84, no. 6, 1831– 1841.

**Author Statement**

Daniela Famiani: Conceptualization, Methodology, Formal analysis, Investigation, Writing - Original Draft, Writing - Review & Editing
Carlo Alberto Brunori: Conceptualization, Investigation, Writing - Original Draft, Supervision
Luca Pizzimenti: Investigation
Fabrizio Cara: Methodology, Formal analysis, Investigation, Writing - Review & Editing

Marco Caciagli: Conceptualization, Resources, Writing - Review & Editing

Laura Melelli: Conceptualization, Resources, Writing - Review & Editing

Francesco Mirabella: Conceptualization, Methodology, Resources, Writing - Review & Editing

Massimiliano R. Barchi: Conceptualization, Resources, Writing - Review & Editing, Supervision

**Declaration of interests**

☒ The authors declare that they have no known competing financial interests or personal relationships that could have appeared to influence the work reported in this paper.

☐The authors declare the following financial interests/personal relationships which may be considered as potential competing interests:

ISTITUTO NAZIONALE
DI GEOFISICA E VULCANOLOGIA

Daniela Famiani
Istituto Nazionale di Geofisica e Vulcanologia – INGV
Sezione di Sismologia e Tettonofisica
Via di Vigna Murata 605
00143 Roma, Italy
email: daniela.famiani@ingv.it

Research article entitled "Geophysical reconstruction of buried geometries and site effects estimation of the Middle Valle Umbra basin (central Italy)" by Famiani D., Brunori, C.A., Pizzimenti, L., Cara F., Caciagli, M., Melelli, L., Mirabella, F. & Barchi, M.R. for consideration for publication in the *Journal of Engineering Geology–Special Issue on Seismic site response estimation for microzonation studies promoting the resilience of urban centers*.

**Highlights**

The subsurface geological setting of an important, active continental basin of Central Italy is reconstructed for the first time, using a multi-technique geophysical approach, mainly based on a campaign of ambient noise measurements

HVNSR contour plots along the two studied transects illustrates both vertical and horizontal variability within the basin succession, offering the possibility of a prompt geological interpretation.

The stratigraphy of the axial (i.e. deeper) part of the basin and the mechanical characteristics of the main layers have been further investigated through two arrays, located at CSA and COST site respectively, producing 1-D velocity models, extended down to the geological bedrock, at an estimated depth of about 800 m

The velocity profiles derived from array analysis were used to convert the resonance frequency of single station measurements into depth for sites with similar stratigraphic setting.